

$c^*$  axis of CE with respect to the compression direction shown in Fig. 3C is that suggested by the optical measurements of Trommsdorff and Wenk (8) and favored in the mechanism of Coe (4) (compare Fig. 3C with Fig. 2). Comparison with our own optical measurements establishes that Z does lie in the obtuse angle between  $c$  and  $a$ .

In addition to the lamellae in the deformed specimens we see a variety of dislocations, most of which lie in the (100) planes of the boundaries of the lamellae. These probably reduce the strain energy due to atomic mismatch of the two phases, and may possibly assist in the transformation. Their Burgers vectors have not yet been determined. Dislocations are also required to accomplish the additional plastic strain which occurs during deformation because of the constraints imposed by the relatively rigid end pieces and because of the effects of friction at the surface of the specimen.

Further work is needed to clarify the nature of the dislocations and to better understand their role, if any, in the transformation mechanism. In addition, the angle of shear associated with the transition has not been determined. This would require the measurement of the angle through which some marker line [ $u0w$ ] (with  $u \neq 0$ ) in the (010) plane is rotated by the transformation of OE to CE. Finally, we do not know yet whether the transformation of CE back to OE can proceed by a coherent mechanism which is the reverse of that for the transformation of OE to CE.

R. S. COE

Earth Sciences Board, University of California, Santa Cruz 95060

W. F. MULLER\*

Department of Materials Science and Engineering, University of California, Berkeley 94720

#### References and Notes

1. F. J. Turner, H. Heard, D. T. Griggs, *Int. Geol. Congr. Rep. Sess. Norden 21st* (1960), part 18, p. 399.
2. C. B. Raleigh, *Science* **150**, 739 (1965); I. Borg and J. Handin, *Tectonophysics* **3**, 249 (1966); R. E. Riecker and T. P. Rooney, *Geol. Soc. Amer. Bull.* **78**, 1045 (1967); J. L. Munoz, *Carnegie Inst. Washington Yearb.* **66**, 369 (1968); C. B. Raleigh, S. H. Kirby, N. L. Carter, H. G. Avé Lallemant, *J. Geophys. Res.* **76**, 4011 (1971).
3. C. B. Sclar, L. C. Carrison, C. M. Schwartz, *Trans. Amer. Geophys. Union* **45**, 121 (1964); F. R. Boyd and J. L. England, *Carnegie Inst. Washington Yearb.* **64**, 117 (1965); J. Grover, *Trans. Amer. Geophys. Union* **53**, 539 (1972).
4. R. S. Coe, *Contrib. Mineral. Petrol.* **26**, 247 (1970).
5. C. M. Wayman, *Introduction to the Crystallography of Martensitic Transformations* (Macmillan, New York, 1964), p. 162. In these respects, the ortho- to clino-transition in enstatite is like the transition from hexagonal close-packed to face-centered cubic stacking in cobalt (see text).

6. W. L. Brown, N. Morimoto, J. V. Smith, *J. Geol.* **69**, 609 (1961).
7. J. Starkey, *Contrib. Mineral. Petrol.* **19**, 133 (1968).
8. V. Trommsdorff and H.-R. Wenk, *ibid.*, p. 158.
9. W. A. Deer, R. A. Howie, J. Zussman, *Rock Forming Minerals* (Longmans, London, 1963), vol. 2, p. 28.
10. J. V. Smith, *Mineral. Soc. Amer. Spec. Pap. No. 2* (1969), p. 3.
11. D. H. Lindsley and J. L. Munoz, *Carnegie Inst. Washington Yearb.* **67**, 86 (1969).
12. D. T. Griggs, *Geophys. J. Roy. Astron. Soc.* **14**, 19 (1967). Our apparatus is a later version, similar to but not exactly the same as that described in this article.
13. These are the optical properties that previous workers (1, 2) have used to identify CE produced by shearing. In addition, we have checked the x-ray powder diffraction pattern for our CE. It is essentially the same as that listed in the powder diffraction file of the American Society for Testing Materials for "low" CE, and determined by D. A. Stephenson, C. B. Sclar, and J. V. Smith [*Mineral. Mag.* **35**, 838 (1966)].
14. R. Castaing, *Rev. Met. Paris* **52**, 669 (1955); J. D. Barber, *J. Mater. Sci.* **5**, 1 (1970); S. V. Radcliffe, A. H. Heuer, R. M. Fisher, J. M. Christie, D. T. Griggs, *Geochim. Cosmochim. Acta* **1** (Suppl. 1), 731 (1970); H. Bach, *J. Non-Cryst. Solids* **3**, 1 (1970). The electron microscopy was done with the Hitachi HV 650 instrument at the University of California, Berkeley, in the laboratory of G. Thomas.
15. These deformation experiments were kindly carried out by H.-R. Wenk at the University of California, Berkeley, at strain rates of  $10^{-4}$  and  $10^{-5}$  sec $^{-1}$ . Because (100) was almost normal to the compression direction, the resolved shear stress on (100) was low and the transformation to CE less developed.
16. Reflections which are systematically extinct or very weak in an x-ray precession photograph are often present in the corresponding electron diffraction pattern because of the phenomenon of multiple reflection [K. W. Andrews, D. J. Dyson, S. R. Keown, *Interpretation of Electron Diffraction Patterns* (Plenum, New York, 1967)]. Thus, in Fig. 3C we see reflections corresponding to (100) planes of CE (bright spots, 9 Å spacing) and (100) planes of OE [weak spots where they do not coincide with (100) planes of CE, 18 Å spacing], whereas they are absent in x-rays precession photographs (8).
17. R.S.C. acknowledges support by NSF grant GA-25165 and an Alfred P. Sloan Foundation fellowship, and thanks H. M. Snyder for help with the deformation experiments. W.F.M. thanks the Deutsche Forschungsgemeinschaft for his research stipend, acknowledges support by the U.S. Atomic Energy Commission through the Lawrence Radiation Laboratory, Berkeley, and is greatly indebted to G. Thomas for hospitality and advice during his stay at Berkeley.

\* Present address: Mineralogische Institut der Universität Frankfurt, Institut für Kristallographie, D-6 Frankfurt a.M., Germany.

25 October 1972; revised 18 January 1973

## Teleconnections in the Equatorial Pacific Ocean

**Abstract.** *Geostrophic water transport by the equatorial countercurrent is compared with the observed sea level difference between two pairs of islands situated north and south of the current. The high correlation between the transport and the sea level difference makes it possible to construct a time series for the countercurrent transport over a 21-year period. The countercurrent carries warm water into the eastern tropical Pacific, and fluctuations in its strength give rise to temperature anomalies off Central America. Periods of exceptionally high transport by the countercurrent in the western Pacific coincide with the occurrence of El Niño several thousand kilometers downstream and demonstrate the existence of teleconnections between events in the Pacific Ocean.*

The transport of ocean water by a major ocean current such as the equatorial countercurrent can be monitored by such simple measurements as those of sea level on its northern and southern flanks. Fluctuations in the transport have a pronounced effect on temperatures off Central America. When transport is strong for a period of several months it contributes to the occurrence of El Niño off Peru (1). Such teleconnections have been found in the atmosphere by Bjerknes (2) but, I believe, have not before been established in the ocean.

The equatorial countercurrent flows eastward between about 4°N and 10°N across the entire Pacific Ocean, transporting warm water from west to east. The flow in the countercurrent is in approximate geostrophic balance (3) and occurs between a ridge near 4°N and a trough near 10°N in the sea surface topography (4). The average rate of transport decreases almost lin-

early from 40 megatons per second in the west to 10 megatons per second in the east (5), but individual values are highly variable. The associated difference in the height of sea level between the ridge and the trough varies between about 30 and 10 cm (6).

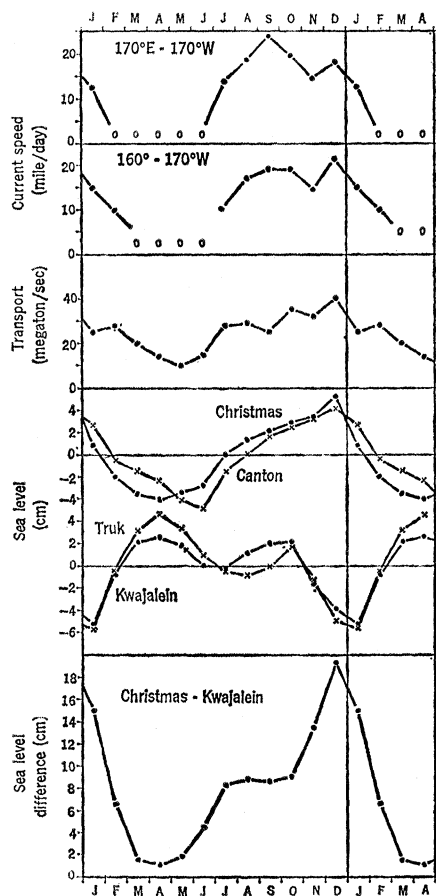
This geostrophic sea level difference can be measured by means of sea level gauges on islands situated in the topographic trough on the northern flank of the countercurrent and in the ridge on its southern flank. A strong relationship exists between the flow in the countercurrent and the sea level difference at stations near the equator and near 10°N (7). There are only two sea level stations near the equator, Christmas Island (2°N, 157°W) and Canton Island (3°S, 172°W). A good correlation ( $r = 0.85$ ) exists between values of the monthly mean sea level at the two stations for a period of 12 years, when simultaneous records are available. The mean seasonal variation shown in Fig.

Fig. 1. Mean seasonal variations of the surface speed of the equatorial countercurrent, its transport, the sea level on both sides, and the sea level difference across it.

1 is  $\pm 4$  cm. Because sea level in the vicinity of the equator is dynamically constrained to have only small meridional slopes, these two stations adequately represent the variations of sea level at the topographic ridge.

There are also two island stations for sea level observations situated near the trough on the northern flank of the countercurrent, Kwajalein ( $9^{\circ}\text{N}$ ,  $168^{\circ}\text{E}$ ) and Truk ( $7^{\circ}\text{N}$ ,  $152^{\circ}\text{E}$ ). The sea level at these two stations (Fig. 1) also has a marked seasonal variation with an amplitude of about  $\pm 5$  cm. The records of monthly mean sea level at the two stations correlate well ( $r=0.77$ ), and can be considered to represent sea level in the trough on the northern flank of the countercurrent.

The sea level difference between Christmas and Kwajalein, shown in Fig. 1 relative to an arbitrary zero point, exhibits a marked seasonal variation with a minimum in March, April, and May, and a maximum (18 cm higher) in December. This seasonal variation of the slope agrees well with the seasonal variation of countercurrent transport as determined from the hydrographic sections and temperature sections across the countercurrent published by Kendall (6). His data were averaged for each month between longitudes  $150^{\circ}\text{W}$  and  $160^{\circ}\text{E}$  in order



to produce the curve shown in Fig. 1. The 39 individual transport computations correlate with  $r=0.59$  with the sea level difference across the current for the corresponding months, which is very high considering that sea level may fluctuate appreciably during each month. Surface current speeds of the

countercurrent were also evaluated for two longitude intervals from the "Atlas of surface currents, northwestern Pacific Ocean" (8). During the period from March to June the number of current vectors showing flow to the west often exceeds the number of those showing flow to the east, and no determination of the speed of the countercurrent is possible. These cases are indicated by open circles in Fig. 1.

Having established the close seasonal correspondence of the sea level difference across the countercurrent, as measured by sea level gauges, with the flow in the countercurrent, I can now reconstruct a time series for ocean water transport by the countercurrent. For this purpose the relative sea level difference across the countercurrent is shown in Fig. 2 by monthly mean values and by a 12-month running mean, for the 21-year period from 1950 to 1970. The difference was formed between the average of the sea level at Canton (observed from 1949 to 1967) and Christmas (1956 to 1970) and the average of the sea level at Truk (1953 to 1971) and Kwajalein (1946 to 1971). Whenever an observation at one station was missing, the average was replaced by the observed value at the other station of the pair, a procedure made possible because of the strong correlation between the stations comprising a pair.

This time series of sea level difference across the countercurrent, which is interpreted as representing the countercurrent transport, shows remarkable fluctuations in height, which are con-

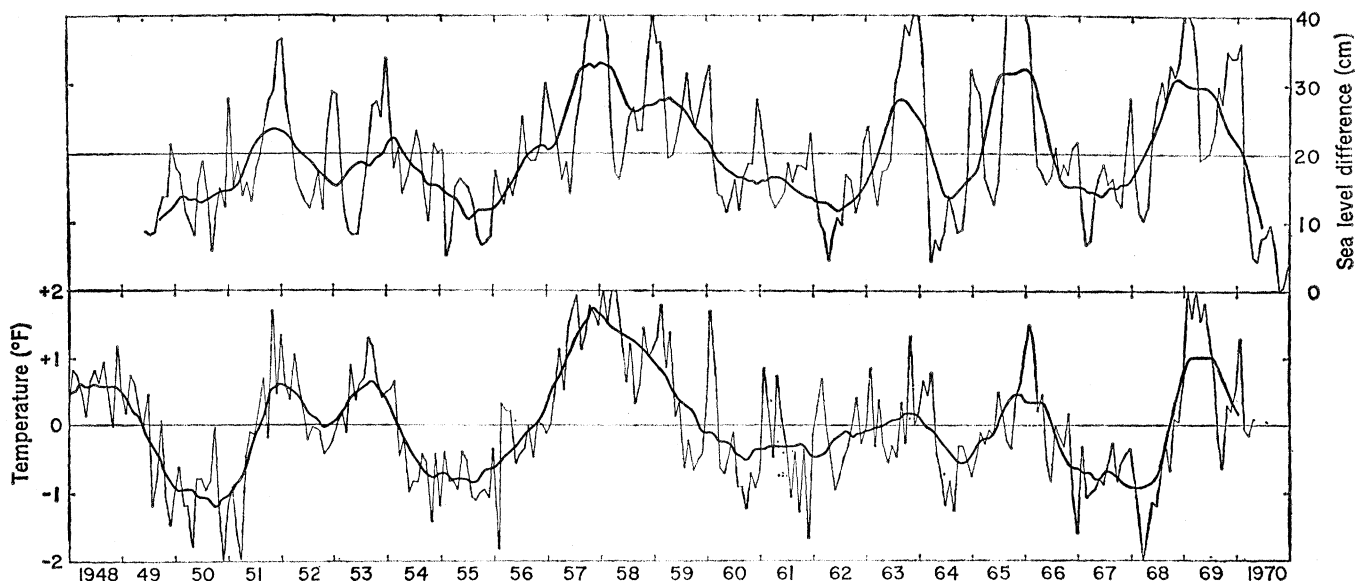


Fig. 2. Time series (1948 to 1970) of (top) the sea level difference across the equatorial countercurrent and (bottom) the sea surface temperature anomaly off Central America. Thin curves give the monthly mean values, heavy curves the 12-month running mean.

sistent for periods of several months and correspond to known anomalous periods in the oceanic and atmospheric climate. If the mean sea level difference between the topographic ridge and trough is set arbitrarily at 20 cm, the highest difference (50 cm) is observed in December 1957, when a strong El Niño developed off Peru (9). Also the 12-month running mean of the sea level difference fluctuates considerably between a high value of 33 cm in January 1958 and a low value of 10 cm in June 1970 and July 1955, the latter recognized as a cold year in the North Pacific (10).

Since the countercurrent transports warm water from the western Pacific Ocean into the eastern tropical Pacific, a strong flow in the countercurrent should lead to an accumulation of warm surface water off the coast of Central America. To study this hypothesis, sea surface temperature anomalies in the triangle formed by the coast of Central America, 100°W longitude, and 10°N latitude were averaged. The data have been published in the form of average monthly anomalies for 2-degree squares (11). The time series of these surface temperature anomalies for individual months and the 12-month running mean are shown in Fig. 2. They correlate well with the countercurrent transport ( $r = 0.79$ ) for the 12-month running means.

The high correlation between the transport of the countercurrent, as inferred from the observed sea level difference across it, and the sea surface temperature anomaly off Central America points to a causal relationship: strong transports in the countercurrent cause an accumulation of warm water in the eastern tropical Pacific. The peaks in the curve of the individual monthly values—especially in the last decade, when observations of sea surface temperatures were more numerous and the averages more reliable—indicate that a positive temperature anomaly follows a peak in the countercurrent transport by about 3 months. This means that the countercurrent must be strong for an appreciable period of time before an effect on the surface temperature in the eastern Pacific Ocean becomes evident, so that it may be possible to use observed sea level differences to predict temperature trends thousands of kilometers downstream. Bjerknes (9) has stressed the importance of the accumulation of large amounts of warm water in the eastern tropical Pacific as a prerequisite for the formation of El Niño.

One should not, however, disregard the possibility that extremes in both the sea surface temperature and the countercurrent transport are simultaneously associated with an anomaly of oceanic and atmospheric circulation over a much larger part of the Pacific.

The major peaks in the strength of the countercurrent are followed by documented occurrences of El Niño off Peru. The most pronounced event is the well-documented El Niño of 1957 and 1958 which coincided with a strong countercurrent transport (12). El Niño in 1953–1954 is mentioned by Posner (13), and the abnormally warm temperatures of Central America in 1965–1966 and in 1969 are both described as El Niño in the monthly bulletins of the fishery-oceanography center in La Jolla (11). The peak in countercurrent transport of 1963–1964 was probably too weak to produce El Niño, and so was the peak in 1951–1952, which apparently did not lead to El Niño, although Schell (14) includes the data from that year in a study of abnormally warm conditions off Peru.

The foregoing demonstrates that changes in the transport of the equatorial countercurrent decisively affect the temperature distribution in the eastern tropical Pacific, and are strongly linked with such climatic abnormalities as El Niño. It is significant that the transport of a major ocean current can be monitored by very simple measure-

ments such as those of sea level, and this fact emphasizes the importance of obtaining long time series representative of climatic fluctuations.

KLAUS WYRTKI

Department of Oceanography,  
University of Hawaii,  
Honolulu 96822

#### References and Notes

1. El Niño is a flow of warm tropical surface water which in some years extends over the cooler waters along the coast of Peru. Its biological consequences lead to a mass mortality of fish and sea birds. It is named El Niño (The Child) because it occurs after Christmas.
2. J. Bjerknes, *Mon. Weather Rev.* **97**, 163 (1969).
3. J. A. Knauss, in *The Sea*, M. N. Hill, Ed. (Interscience, New York, 1963), vol. 1, pp. 235–252.
4. J. L. Reid, *Tellus* **13**, 489 (1961).
5. K. Wyrtki and R. Kendall, *J. Geophys. Res.* **72**, 2073 (1967).
6. R. Kendall, dissertation, Nova University, Fort Lauderdale, Florida (1970).
7. The values of monthly mean sea level were obtained from the National Ocean Survey, National Oceanic and Atmospheric Administration, Rockville, Maryland.
8. "Atlas of surface currents, northwestern Pacific Ocean," *U.S. Navy Hydrogr. Off. Publ.* 569 (1953).
9. J. Bjerknes, *Bull. Inter.-Amer. Trop. Tuna Comm.* **5**, 219 (1961).
10. M. Rodewald, *Deut. Hydrogr. Z.* **11**, 78 (1958).
11. *Fishing Information*, issued monthly by National Marine Fisheries Service, La Jolla, California.
12. T. S. Austin, *Calif. Coop. Oceanic Fish. Invest. Rep.* **7**, 52 (1960).
13. G. S. Posner, *Bull. Bingham Oceanogr. Collect. Yale Univ.* **16**, 105 (1957).
14. I. I. Schell, *J. Geophys. Res.* **70**, 5529 (1965).
15. Supported by the National Science Foundation and the Office of Naval Research under the North Pacific Experiment of the International Decade of Ocean Exploration; this support is gratefully acknowledged. Hawaii Institute of Geophysics Contribution No. 514.

7 December 1972; revised 26 January 1973 ■

## Lunar Cinder Cones

*Abstract. Data on terrestrial eruptions of pyroclastic material and ballistic considerations suggest that in the lunar environment (vacuum and reduced gravity) low-rimmed pyroclastic rings are formed rather than the high-rimmed cinder cones so abundant on the earth. Dark blanketing deposits in the Taurus-Littrow region (Apollo 17 landing area) are interpreted as being at least partly composed of lunar counterparts of terrestrial cinder cones.*

Mantling deposits with low albedos (.074 to .085) (1) have been mapped in several regions of the moon (Aristarchus Plateau, Copernicus CD, the Rima Bode area, Alphonsus, Sulpicius Gallus, Littrow, and north of Hyginus) and have generally been interpreted as pyroclastics because of their low albedos and smooth surfaces and the way that they subdue underlying terrain (2). Possible lunar pyroclastic cones have been described in other areas, most notably in the Marius Hills (3). However, a puzzling aspect of the dark mantle deposits is that they do not appear to be associated with

cinder cones of the size and type of those found amid, and constituting the source of, terrestrial pyroclastic deposits. As they often mantle relatively young deposits, these units may represent some of the youngest stages of igneous activity recognized on the lunar surface. An area in the dark mantle near the crater Littrow (Fig. 1A) was chosen as the landing site for the Apollo 17 mission, and a primary objective of the mission was to explore and sample the low-albedo material.

Before Apollo 17, significant new information relevant to the nature of the sources of these dark mantle deposits